Journal of Materials Chemistry

Cite this: J. Mater. Chem., 2012, 22, 17709

www.rsc.org/materials

PAPER

Synthesis and photovoltaic properties of benzo[1,2-*b*:4,5-*b*′]dithiophene derivative-based polymers with deep HOMO levels†

Heung Gyu Kim,‡[a] Sae Byeok Jo,‡[a] Chiyeoung Shim,[a] Jaewon Lee,[a] Jisoo Shin,[a] Eun Chul Cho,[b] Soo-Ghang Ihn,[c] Yeong Suk Choi,[c] Yungi Kim[c] and Kilwon Cho*[a]

Received 21st April 2012, Accepted 23rd June 2012
DOI: 10.1039/c2jm32514d

Two benzo[1,2-*b*:4,5-*b*′]dithiophene (BDT) derivatives with conjugated substituents, triisopropylsilylethynyl (TIPS) and 4-octylphenylethynyl groups, were synthesized as donor units (D) and copolymerized with two acceptor units (A), 4,7-bis(4-octylthiophen-2-yl)-2,1,3-benzothiadiazole (BT) and 4,4′-diundecyl-2,2′-bithiazole (BTZ), respectively, using Stille coupling reaction to afford four new copolymers, **PTBDT-BT**, **PTBDT-BTZ**, **POPEBDT-BT**, **POPEBDT-BTZ**. All polymers exhibited highest occupied molecular orbital (HOMO) energy levels that were deeper than −5.4 eV due to the conjugated substituents. Small band gaps were successfully achieved for **PTBDT-BT** (1.67 eV) and **POPEBDT-BT** (1.67 eV) and were attributable to the strong intramolecular charge transfer within the D–A alternating structure. The resultant photovoltaic performances showed high open-circuit voltages (V_{oc}) ranging from 0.73 V to 0.92 V, whereas the power conversion efficiencies (PCEs) depended strongly on the blend morphologies. The polymer solar cell based on the blend of **PTBDT-BT** and $PC_{71}BM$ gave the best photovoltaic performance among the series, with a high V_{oc} of 0.81 V and a PCE of 4.61%.

1. Introduction

Conjugated polymer solar cells have attracted interest as possible candidates for realizing lightweight flexible energy sources with low costs and large-area fabrication.[1–3] Until recently, bulk heterojunction (BHJ)-based polymer solar cells prepared from blends of conjugated donor polymers and (6,6)-phenyl-C_{61}-butyric acid methyl ester (PCBM) as the acceptor have yielded the most successful enhancement in the power conversion efficiency (PCE).[4] Among the many electron-donating conjugated polymers developed thus far, highly crystalline poly(3-hexylthiophene) (P3HT) has been the most widely studied donor polymer, reaching PCEs of up to 5% in the presence of an optimized active layer morphology prepared *via* a variety of post-treatment techniques.[5–9] Despite the successful optimization of the active layer characteristics, device PCEs must be enhanced to at least 10% before practical applications become feasible. The limited range (300–650 nm) of the visible light absorption profile and the high HOMO energy level (−5.0 eV) of P3HT have hindered further enhancements of the photovoltaic performances.

In this sense, tremendous efforts have been devoted toward developing new small band gap polymers with deep HOMO energy levels, and several design rules for this purpose have been proposed thus far. An alternating copolymer structure with electron-rich (donor, D) and electron-deficient (acceptor, A) repeating units has been shown to provide the most effective strategy for adjusting the optical and electrical properties of copolymers *via* intramolecular charge transfer.[10,11] These D–A alternating copolymers were designed to achieve deep HOMO energy levels (<−5.2 eV) toward a high open-circuit voltage (V_{oc}) and a small band gap (<1.9 eV) for efficient sunlight absorption. Numerous electron-rich monomers, such as carbazole,[12] dithienosilole,[13] benzo[1,2-*b*:4,5-*b*′]dithiophene (BDT),[14] *etc.*, and electron-deficient monomers, such as benzothiadiazole,[13] thieno[3,4-*b*]thiophene-2-carboxylate,[15] bithiazole,[16] and thieno[3,4-*c*]pyrrole-4,6-dione,[17–19] *etc.*, were synthesized, and their combinations toward D–A alternating copolymers have been investigated. More comprehensive and systematic investigations that could provide an understanding of the relationship between the molecular structure and properties of D–A alternating copolymers would be required for the further development of finely tuned materials for use in highly efficient polymer solar cells.

Among the recently synthesized D–A copolymers, BDT-based copolymers have attracted the most interest with their promising photovoltaic performances (>7%).[20] BDT units display strong π–π stacking and good hole mobilities due to their high planarity

[a]*Department of Chemical Engineering, Pohang University of Science and Technology, Pohang, 790-784, Korea. E-mail: kwcho@postech.ac.kr*
[b]*Department of Chemical Engineering, Hanyang University, Seong-dong gu, Seoul, 133-791, Korea*
[c]*Samsung Advanced Institute of Technology Samsung Electronics, Yongin, 446-712, Korea*

† Electronic supplementary information (ESI) available. See DOI: 10.1039/c2jm32514d

‡ Heung Gyu Kim and Sae Byeok Jo contributed equally to this work.

and small steric hindrance between adjacent molecules.[14] Alkyl or alkoxy groups are commonly introduced as BDT substituents to increase the solubility of the polymers in organic solvents. The choice of the substituent plays a critical role in controlling the optical and electrical properties of the conjugated polymers; therefore, the electron affinity of a substituent must be carefully considered.[20] The triisopropylsilylethynyl (TIPS) and alkyl phenylethynyl substituents have been used previously to modify acene molecules in organic field effect transistors (OFETs).[21,22] TIPS substituents are more effective in lowering the lowest unoccupied molecular orbital (LUMO) and HOMO energy levels than conventional alkoxy substituents.[23] Moreover, TIPS substituents improve the solubility, π–π stacking, and stability of acene molecules.[21] Another conjugated substituent, the alkyl phenylethynyl group, has been tested in the context of BDT homopolymers and has yielded significant reductions in the HOMO energy level (−5.61 eV) of the polymers. Consequently, high V_{oc} values (0.85 eV) have been obtained from polymer solar cell devices that include PCBM.[24] Yang and coworkers utilized an alkylthiophene substituent on BDT-based copolymers to obtain relatively deep HOMO energy levels (−5.31 eV), a high V_{oc} (0.92 eV), and a PCE of 5.66%.[25] A handful of other studies have reported on the modification of the BDT unit to prepare D–A copolymers;[26,27] however, additional studies are required to optimize the properties of BDT-based copolymers.

In this work, we modified a BDT unit by introducing two substituents with different conjugation lengths, TIPS and 4-octylphenylethynyl groups, into the central benzene ring, with the aim of lowering the HOMO energy levels of the BDT unit and, consequently, the HOMO energy levels of the D–A copolymers comprising the modified BDT unit. Because the HOMO energy levels of D–A copolymers are mainly determined by the HOMO energy level of the donor unit, a significant reduction in the HOMO energy levels of the modified BDT-based copolymers was expected. As shown in Scheme 1, 4,8-bis((triisopropylsilyl)ethynyl)benzo[1,2-*b*:4,5-*b*′]dithiophene (**TBDT**) and 4,8-bis((4-octylphenyl)ethynyl)benzo[1,2-*b*:4,5-*b*′]dithiophene (**OPEBDT**) were synthesized as donor monomers. These monomers were each copolymerized with two electron-deficient monomers, 4,7-bis(4-octylthiophen-2-yl)-2,1,3-benzothiadiazole (BT, strong acceptor) and 4,4′-diundecyl-2,2′-bithiazole (BTZ, weak acceptor). Four new copolymers, **PTBDT-BT**, **PTBDT-BTZ**, **POPEBDT-BT**, and **POPEBDT-BTZ**, were successfully synthesized by Stille coupling reaction, as shown in Scheme 2. We demonstrated that the HOMO energy levels of the polymers were successfully lowered *via* modification of the BDT unit. A high V_{oc} for photovoltaic devices comprising the synthesized polymers was achieved, up to 0.92 V. The synthesis, characterization, and photovoltaic properties of these polymers were thoroughly investigated.

2. Experimental

Materials

All reagents were purchased from Aldrich, TCI, and Acros, and were used without further purification. All anhydrous organic solvents for the synthesis and device fabrication steps, including tetrahydrofuran (THF), chloroform, toluene,

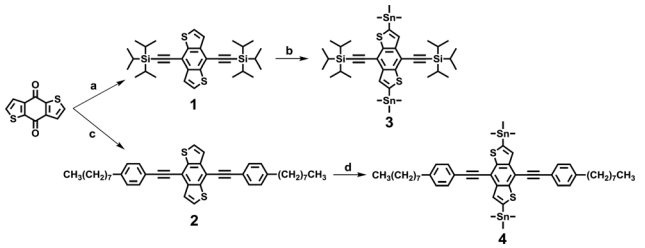

Scheme 1 Synthetic route for the monomers. *Reagents and conditions*: (a) **1**: ((triisopropylsilyl)ethynyl)magnesium chloride, THF, 60 °C; **2**: $SnCl_2 \cdot 2H_2O$, 10% HCl, 60 °C, 57%; (b) **1**: *n*-BuLi, THF, −78 °C; **2**: Me_3SnCl, RT, 80%; (c) **1**: ((4-octylphenyl)ethynyl)magnesium chloride, THF, 60 °C; **2**: $SnCl_2 \cdot 2H_2O$, 10% HCl, 60 °C, 72%; and (d) **1**: *n*-BuLi, THF, −78 °C; **2**: Me_3SnCl, RT, 80%.

N,*N*-dimethylformamide (DMF), chlorobenzene (CB), and 1,2-dichlorobenzene (DCB), were purchased from Aldrich. The monomers, 4,7-bis(4-octylthiophen-2-yl)-2,1,3-benzothiadiazole[28] and 5,5′-dibromo-4,4′-diundecyl-2,2′-bithiazole,[29] were synthesized according to modified literature procedures.

Measurements

^1H and ^{13}C NMR spectra were recorded on a Bruker AVANCE 400 spectrometer operated at 400 MHz and 100 MHz in chloroform-d solutions. The number-average (M_n) and weight-average (M_w) molecular weights were measured by gel permeation chromatography (GPC, Shimadzu) using chloroform as the eluent and a calibration curve of polystyrene standards at 40 °C. UV-Visible absorption spectra were measured using a Varian CARY-5000 UV/Visible spectrophotometer. Differential scanning calorimetric (DSC) and thermogravimetric analysis (TGA) measurements of the polymers were performed using DSC 2910 (TA Instruments) and TGA 2050 (TA Instruments) instruments under a nitrogen atmosphere at heating and cooling rates of 10 °C min^{-1}. Cyclic voltammograms were recorded using a SP-200 (BioLogic). A 0.1 M tetrabutylammonium hexafluorophosphate (Bu_4NPF_6) solution in acetonitrile was used as

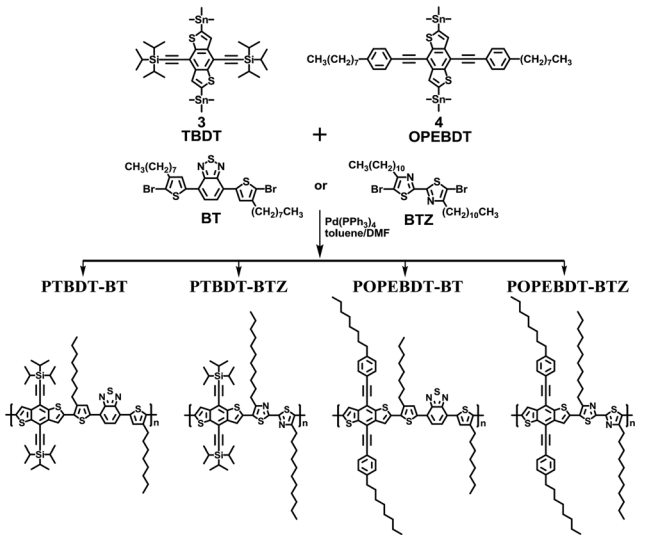

Scheme 2 Synthesis of BDT-based D–A polymers.

the electrolyte solution with a scan rate of 50 mV s^{-1}. A three-electrode system was used, consisting of an Ag/AgCl reference electrode, a glassy carbon working electrode, and a platinum counter electrode. Polymer thin films were formed by drop-casting of the polymer solutions in chloroform onto the working electrode. The potential of the Ag/AgCl reference electrode was internally calibrated using a ferrocene/ferrocenium redox couple (Fc/Fc^+). The energy levels were estimated according to the equations: HOMO = $-(4.80 + E_{onset,\ ox})$ and LUMO = $-(4.80 + E_{onset,\ red})$.[30,31]

4,8-Bis((triisopropylsilyl)ethynyl)benzo[1,2-*b*:4,5-*b*′]dithiophene (1). Isopropylmagnesium chloride (2.0 M in THF, 5.5 mL, 11.0 mmol) was added dropwise to a solution of (triisopropylsilyl) acetylene (1.98 g, 10.86 mmol) in dry THF (10 mL). The solution was stirred at 60 °C for 2 h and cooled to RT. Benzo[1,2-*b*:4,5-*b*′] dithiophene-4,8-dione (0.6 g, 2.72 mmol) was added to the solution, and the mixture was stirred at 60 °C for 8 h. After cooling to RT, $SnCl_2 \cdot 2H_2O$ (2.0 g, 8.86 mmol) and a 10% aq. HCl solution (2 mL) were added carefully to the solution. The reaction mixture was refluxed at 60 °C for 5 h. After the reaction, the solution was poured into water (300 mL), and dichloromethane (300 mL) was added. The organic layer was washed with water (300 mL × 3) and dried over $MgSO_4$. After removal of the solvent, the residue was purified by column chromatography on silica gel using hexane as the eluent to afford a greenish solid. Yield: 0.86 g (57%). ^{1}H NMR (400 MHz, $CDCl_3$), δ (ppm): 7.61 (d, 2H), 7.56 (d, 2H), 1.24 (m, 42H). ^{13}C NMR (100 MHz, $CDCl_3$), δ (ppm): 140.87, 138.51, 128.28, 123.15, 112.19, 102.64, 101.62, 18.78, 11.33. Elemental analysis: calc. for $C_{32}H_{46}S_2Si_2$: C, 69.75; H, 8.41; S, 11.64. Found: C, 69.98; H, 8.17; S, 11.44%.

4,8-Bis((4-octylphenyl)ethynyl)benzo[1,2-*b*:4,5-*b*′]dithiophene (2). Isopropylmagnesium chloride (2.0 M in THF, 5.0 mL, 10.0 mmol) was added dropwise to a solution of (4-octylphenyl) acetylene (2.0 g, 9.33 mmol) in dry THF (10 mL). The solution was stirred at 60 °C for 2 h and cooled to RT. Benzo[1,2-*b*:4,5-*b*′] dithiophene-4,8-dione (0.5 g, 2.27 mmol) was added to the solution, and the mixture was stirred at 60 °C for 8 h. After cooling to RT, $SnCl_2 \cdot 2H_2O$ (2.0 g, 8.86 mmol) and a 10% aq. HCl solution (2 mL) were added carefully to the solution. The reaction mixture was refluxed at 60 °C for 5 h. After the reaction, the solution was poured into water (300 mL), and dichloromethane (300 mL) was added. The organic layer was washed with water (300 mL × 3) and dried over $MgSO_4$. After removal of the solvent, the residue was purified by column chromatography on silica gel using hexane–chloroform (1 : 1, v/v) as an eluent to afford an orange solid. Yield: 1.0 g (72%). ^{1}H NMR (400 MHz, $CDCl_3$), δ (ppm): 7.72 (d, 2H), 7.61 (d, 4H), 7.59 (d, 2H), 7.24 (d, 4H), 2.65 (t, 4H), 1.62 (quintet, 4H), 1.30 (m, 20H), 0.89 (t, 6H). ^{13}C NMR (100 MHz, $CDCl_3$), δ (ppm): 144.18, 140.28, 138.19, 131.71, 128.63, 128.02, 123.28, 120.01, 112.09, 99.49, 85.13, 36.02, 31.89, 31.30, 29.47, 29.28, 29.27, 22.68, 14.12. Elemental analysis: calc. for $C_{42}H_{46}S_2$: C, 82.03; H, 7.54; S, 10.43. Found: C, 81.86; H, 7.60; S, 10.21%.

2,6-(Trimethyltin)-4,8-bis((triisopropylsilyl)ethynyl)benzo[1,2-*b*:4,5-*b*′]dithiophene (3). Compound **1** (0.6 g, 1.09 mmol) was dissolved in dry THF (40 mL) and cooled to −78 °C before adding *n*-BuLi (1.6 M in hexane, 1.5 mL, 2.4 mmol). After stirring at −78 °C for 1 h, trimethyltin chloride (1.0 M in THF, 2.4 mL, 2.4 mmol) was added in one portion. The solution was stirred overnight and allowed to reach RT. After the reaction, the solution was diluted with dichloromethane (200 mL), washed with water (300 mL × 3), and dried over $MgSO_4$. The organic phase was concentrated to 10 mL, and methanol was poured over the solution to yield a yellow solid. Yield: 0.77 g (80%). ^{1}H NMR (400 MHz, $CDCl_3$), δ (ppm): 7.68 (s, 2H), 1.24 (m, 42H), 0.46 (s, 18H). ^{13}C NMR (100 MHz, $CDCl_3$), δ (ppm): 144.68, 143.50, 139.63, 131.10, 110.36, 103.34, 100.64, 18.80, 11.38, −8.37. Elemental analysis: calc. for $C_{38}H_{62}S_2Si_2Sn_2$: C, 52.06; H, 7.13; S, 7.32. Found: C, 52.34; H, 7.07; S, 7.38%.

2,6-(Trimethyltin)-4,8-bis((4-octylphenyl)ethynyl)benzo[1,2-*b*:4,5-*b*′]dithiophene (4). Compound **4** was prepared using a procedure similar to that described for the synthesis of compound **3**. Yield: 0.61 g (80%). ^{1}H NMR (400 MHz, $CDCl_3$), δ (ppm): 7.75 (s, 2H), 7.62 (d, 4H), 7.24 (d, 4H), 2.65 (t, 4H), 1.62 (quintet, 4H), 1.30 (m, 20H), 0.91 (t, 6H), 0.49 (s, 18H). ^{13}C NMR (100 MHz, $CDCl_3$), δ (ppm): 144.53, 143.95, 143.36, 138.99, 131.75, 130.95, 128.58, 120.30, 110.21, 98.76, 85.75, 36.01, 31.89, 31.32, 29.48, 29.27, 22.68, 14.12, −8.24. Elemental analysis: calc. for $C_{48}H_{62}S_2Sn_2$: C, 61.29; H, 6.64; S, 6.82. Found: C, 61.47; H, 6.78; S, 6.75%.

Poly{4,8-bis((triisopropylsilyl)ethynyl)benzo[1,2-*b*:4,5-*b*′]dithiophene-*alt*-4,7-bis(4-octylthiophen-2-yl)-2,1,3-benzothiadiazole-5,5′-diyl} (PTBDT-BT). Compound **3** (0.3 g, 0.34 mmol), 4,7-bis-(5-bromo-4-octylthiophen-2-yl)-2,1,3-benzothiadiazole (0.23 g, 0.34 mmol), and $Pd(PPh_3)_4$ (15 mg) were dissolved in a mixture of toluene (15 mL) and DMF (2 mL). The reaction flask was purged with nitrogen for 2 h. The solution was refluxed for 3 days at 120 °C, and then cooled to RT. The polymer solution was poured into methanol (200 mL). The resulting blue-black solid was filtered and Soxhlet extracted with methanol, acetone, hexane, and chloroform until the wash solution of each extraction was colorless. The chloroform fraction was concentrated and poured into methanol, filtered, and dried under vacuum. Yield: 0.28 g (76%). ^{1}H NMR (400 MHz, $CDCl_3$), δ (ppm): 8.12–7.25 (m, 6H), 2.98–2.72 (br, 4H), 1.82–1.10 (br, 66H), 0.90 (br, 6H). GPC ($CHCl_3$, 40 °C): M_n = 15.4 kg mol^{-1}, M_w = 25.7 kg mol^{-1}, PDI = 1.67.

Poly{4,8-bis((triisopropylsilyl)ethynyl)benzo[1,2-*b*:4,5-*b*′]dithiophene-*alt*-4,4′-diundecyl-2,2′-bithiazole} (PTBDT-BTZ). **PTBDT-BTZ** was synthesized using the procedure described for the synthesis of **PTBDT-BT**. Compound **3** (0.4 g, 0.46 mmol) and 5,5′-dibromo-4,4′-diundecyl-2,2′-bithiazole (0.29 g, 0.46 mmol) were used as the monomers. Yield: 0.43 g (92%). ^{1}H NMR (400 MHz, $CDCl_3$), δ (ppm): 7.83–7.72 (br, 2H), 3.10–2.77 (br, 4H), 1.89–1.76 (br, 4H), 1.47–1.22 (br, 74H), 0.87 (br, 6H). GPC ($CHCl_3$, 40 °C): M_n = 13.6 kg mol^{-1}, M_w = 27.5 kg mol^{-1}, PDI = 2.02.

Poly{4,8-bis((4-octylphenyl)ethynyl)benzo[1,2-*b*:4,5-*b*′]dithiophene-*alt*-4,7-bis(4-octylthiophen-2-yl)-2,1,3-benzothiadiazole-5,5′-diyl} (POPEBDT-BT). **POPEBDT-BT** was synthesized using the procedure described for the synthesis of **PTBDT-BT**.

Compound **4** (0.3 g, 0.32 mmol) and 4,7-bis(5-bromo-4-octylthiophen-2-yl)-2,1,3-benzothiadiazole (0.22 g, 0.32 mmol) were used as the monomers. Yield: 0.27 g (70%). ^{1}H NMR (400 MHz, $CDCl_3$), δ (ppm): 8.11–6.85 (br, 14H), 3.02–2.44 (br, 8H), 1.88–1.65 (br, 8H), 1.28 (br, 40H), 0.92–0.85 (m, 12H). GPC ($CHCl_3$, 40 °C): M_n = 9.2 kg mol^{-1}, M_w = 14.4 kg mol^{-1}, PDI = 1.56.

Poly{4,8-bis((4-octylphenyl)ethynyl)benzo[1,2-*b*:4,5-*b*′]dithiophene-*alt*-4,4′-diundecyl-2,2′-bithiazole} (POPEBDT-BTZ). **POPEBDT-BTZ** was synthesized using the procedure described for the synthesis of **PTBDT-BT**. Compound **4** (0.28 g, 0.30 mmol) and 5,5′-dibromo-4,4′-diundecyl-2,2′-bithiazole (0.19 g, 0.30 mmol) were used as the monomers. Yield: 0.26 g (80%). ^{1}H NMR (400 MHz, $CDCl_3$), δ (ppm): 7.93–6.73 (br, 10H), 3.15–2.68 (br, 8H), 1.31 (br, 60H), 0.91 (br, 12H). GPC ($CHCl_3$, 40 °C): M_n = 9.4 kg mol^{-1}, M_w = 15.7 kg mol^{-1}, PDI = 1.67.

Fabrication and characterization of the polymer solar cells

An ITO patterned glass (15 Ω sq^{-1}) was cleaned by sonication with warm acetone and isopropyl alcohol, followed by UV-ozone treatment. After cleansing, a 10 nm MoO_3 film was formed by depositing and annealing Mo films in the presence of oxygen. $PC_{71}BM$ (99.5%, Solenne Inc.) was used as an acceptor material in this study. The polymer:$PC_{71}BM$ blend solutions were prepared in DCB with various composition ratios and were blended above 60 °C for 2 days with severe agitation. Several devices were fabricated in such a way that 1,8-diiodooctane (DIO) was added to the solution 1 h before film deposition. The blend solutions were then spin-cast onto the MoO_3-coated glasses and dried for 1 h under a N_2 environment, giving a total thickness of 70–120 nm, depending on the concentration of each solution. The ZnO–PEG solutions[32,33] were spin-coated onto the active layers to a thickness of 45 nm and dried under high vacuum (<10^{-6} Torr) for 1 h. On top of these films, Al cathodes were formed by thermal evaporation. In the case of the devices without ZnO–PEG layers, the 6 Å LiF layer was deposited on the active layers by thermal evaporation before the formation of Al electrode. The current–voltage (J–V) characteristics were measured using a Keithley 4200 power source under AM 1.5G illumination at an intensity of 100 mW cm^{-2} (Oriel 1 kW solar simulator) using a PVM 132 reference cell certified by NREL. All electrical measurements and fabrication processes were performed under an inert N_2 environment. The incident photon-to-current conversion efficiency (IPCE) was measured using a photo-modulation spectroscopy setup (Merlin, Oriel) with monochromatic light from a xenon lamp. The power density of the monochromatic light was calibrated using a Si photodiode certified by the National Institute for Standards and Technology (NIST).

3. Results and discussion

Synthesis and thermal stability

The general synthetic route for the monomers (compounds **3** and **4**) is described in Scheme 1. Compounds **1** and **2**, with triisopropylsilylethynyl (TIPS) and 4-octylphenylethynyl substituents, were synthesized by their corresponding Grignard reactions, followed by reduction with $SnCl_2 \cdot 2H_2O$, in good yield (57% and 72%). The resulting compounds were easily lithiated by *n*-BuLi, and then reacted with trimethyltin chloride to afford compounds **3** and **4** in 80% yield. The Stille coupling reaction with a $Pd(PPh_3)_4$ catalyst in toluene/DMF yielded the polymers, as shown in Scheme 2, in which compounds **3** or **4** were used as donor units, and 4,7-bis(4-octylthiophen-2-yl)-2,1,3-benzothiadiazole (BT) or 4,4′-diundecyl-2,2′-bithiazole (BTZ) were used as acceptor units. The resulting polymers were carefully purified through Soxhlet extraction using methanol, acetone, hexane, and chloroform. The chemical structures of the synthesized monomers and polymers were confirmed by NMR spectroscopy. All polymers exhibited good solubility in common organic solvents, such as chloroform, toluene, CB, and DCB. The number-average molecular weights (M_n) and polydispersity indices (PDIs) of the four polymers were measured by gel permeation chromatography (GPC) using chloroform as the eluent and polystyrene as the internal standard. The results are summarized in Table 1. The M_n values for **PTBDT-BT**, **PTBDT-BTZ**, **POPEBDT-BT**, and **POPEBDT-BTZ** were 15.4 kg mol^{-1}, 13.6 kg mol^{-1}, 9.2 kg mol^{-1}, and 9.4 kg mol^{-1}, with PDIs of 1.67, 2.02, 1.56, and 1.67, respectively. **PTBDT-BT** and **PTBDT-BTZ** exhibited higher M_n than **POPEBDT-BT** and **POPEBDT-BTZ** because the **TBDT** molecules containing bulky triisopropylsilylethynyl groups displayed better solubility than **OPBDT**, with the rigid 4-octylphenylethynyl substituents.

The thermal stabilities of the synthesized polymers were measured by TGA, as shown in Fig. 1. The thermal decomposition temperatures (T_d, at 5% weight loss) of **PTBDT-BT**, **PTBDT-BTZ**, **POPEBDT-BT**, and **POPEBDT-BTZ** were 421, 364, 316, and 398 °C, indicating good thermal stability for applications in polymer solar cells, as shown in Table 1. The DSC

Table 1 Intrinsic properties of the synthesized polymers

						UV-vis absorption spectra				Cyclic voltammetry		
						Solution	Film					
Polymer	M_n[a] (kg mol^{-1})	PDI[a]	T_d (°C)	Surface E (mJ m^{-2})	Hole mobility[b] (cm^2 V^{-1} s^{-1})	λ_{max} (nm)	λ_{max} (nm)	λ_{onset} (nm)	E_g^{opt} (eV)[c]	E_{ox}^{onset}/HOMO[d] (V/eV)	E_{red}^{onset}/LUMO[d] (V/eV)	E_g^{EC} (eV)
PTBDT-BT	15.4	1.67	421	33.69	1.93×10^{-3}	544	616	742	1.67	0.62/−5.42	−1.28/−3.52	1.90
PTBDT-BTZ	13.6	2.02	364	20.86	4.34×10^{-5}	485	528, 565	612	2.03	1.11/−5.91	−1.28/−3.52	2.39
POPEBDT-BT	9.2	1.56	316	21.31	4.82×10^{-4}	554	598	742	1.67	0.78/−5.58	−1.27/−3.53	2.05
POPEBDT-BTZ	9.4	1.67	398	28.06	5.66×10^{-4}	531	543	635	1.95	0.84/−5.64	−1.29/−3.51	2.13

[a] Determined by GPC using polystyrene standards in chloroform as the eluent. [b] Calculated from SCLC measurement. [c] Estimated from the onset of the UV-vis spectra measured from thin films. [d] Measured by cyclic voltammetry in a 0.1 M Bu_4NPF_6/CH_3CN solution *vs.* Ag/AgCl.

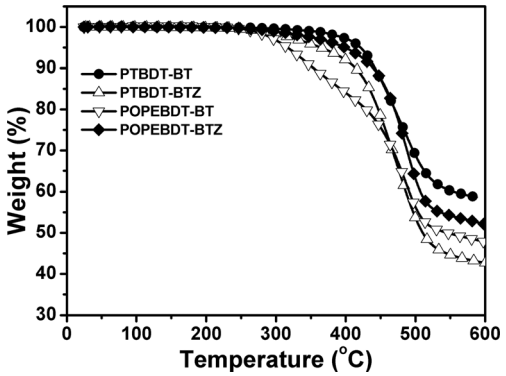

Fig. 1 TGA plots of the polymers with a heating rate of 10 °C min^{-1} under a N_2 atmosphere.

measurements did not reveal endo- or exothermic behavior between 50 °C and 260 °C.

Optical properties

The UV-visible absorption spectra of the polymers were obtained in chloroform solutions and in the thin film state, as shown in Fig. 2. The maximum absorption wavelengths (λ_{max}) and optical band gaps (E_g^{opt}) are summarized in Table 1. The λ_{max}s of **PTBDT-BT**, **PTBDT-BTZ**, **POPEBDT-BT**, and **POPEBDT-BTZ** in solution were observed at 544, 485, 544, and 531 nm, respectively, whereas those of thin films were observed at 616, 565, 598, and 543 nm. The absorption spectra of the polymers were red-shifted in the thin films due to the increased π–π interchain interactions upon aggregation. The optical band gaps (E_g^{opt}, eV) of **PTBDT-BT**, **PTBDT-BTZ**, **POPEBDT-BT**, and **POPEBDT-BTZ** were calculated from an extrapolation of the absorption edges in the thin film states and were found to be 1.67, 2.03, 1.67, and 1.95 eV. The small band gap of 1.67 eV was successfully achieved for **PTBDT-BT** and **POPEBDT-BT** by the strong intramolecular charge transfer effects between the donor units and the acceptor unit (BT), whereas the two conjugated substituents showed only minor effects. The effects of the conjugation length were stronger in the presence of a weak acceptor unit (BTZ). **POPEBDT-BTZ** (1.95 eV) exhibited a smaller band gap than **PTBDT-BTZ** (2.03 eV). On the other hand, **PTBDT-BT** and **POPEBDT-BTZ** displayed a hint of shoulders adjacent to the absorption maxima in the thin film state, possibly due to the formation of intermolecular π–π stacking and the planarization of the backbone.

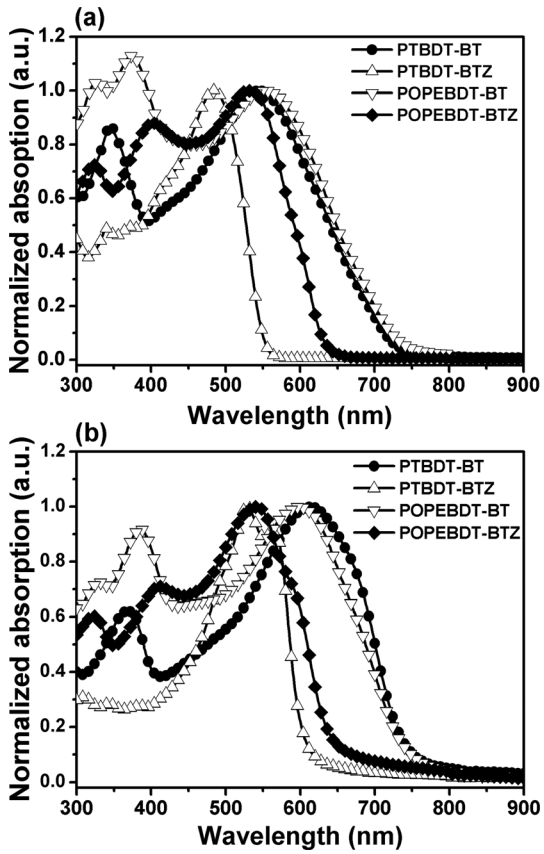

Fig. 2 Normalized absorption spectra of the polymers (a) in chloroform solution and (b) in thin films.

Electrochemical properties

Cyclic voltammetry (CV) was used to investigate the HOMO and LUMO energy levels of the synthesized polymers using a grassy carbon working electrode, a platinum wire counter electrode, and a Ag/AgCl reference electrode in a 0.1 M tetrabutylammonium hexafluorophosphate (Bu_4NPF_6) solution in acetonitrile at a scan rate of 50 mV s^{-1}, and the results are shown in Fig. 3 and Table 1. All polymers exhibited good reversible oxidation and reduction peaks. The HOMO and LUMO energy levels were calculated according to the procedure described in the

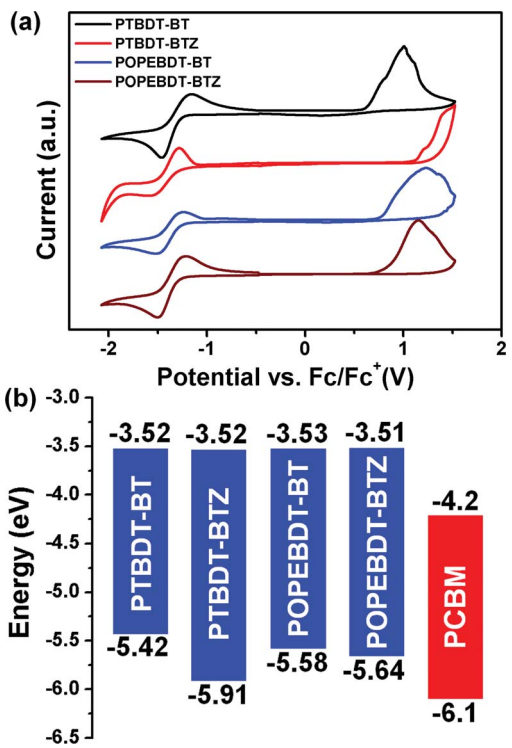

Fig. 3 (a) Cyclic voltammograms of the polymers in the thin films and (b) the energy level diagrams of the polymers.

literature.[30,31] The HOMO energy levels of **PTBDT-BT**, **PTBDT-BTZ**, **POPEBDT-BT**, and **POPEBDT-BTZ** were calculated to be −5.42, −5.91, −5.58, and −5.64 eV, whereas the LUMO energy levels were −3.52, −3.52, −3.53, and −3.51 eV, respectively, with ferrocene as the reference. All synthesized polymers exhibited deep HOMO energy levels (<−5.4 eV) to ensure good air stability and a high V_{oc} in the polymer solar cell applications. **PTBDT-BTZ** and **POPEBDT-BTZ** presented deeper HOMO levels than **PTBDT-BT** and **POPEBDT-BT**. **PTBDT-BTZ** exhibited an especially deep HOMO energy level (−5.91 eV) in comparison with the other synthesized polymers. The LUMO energy levels of the synthesized polymers were about 0.7 eV higher than the LUMO level (−4.2 eV) of PCBM, generating a downhill driving force for the energetically favorable electron transfer reactions.

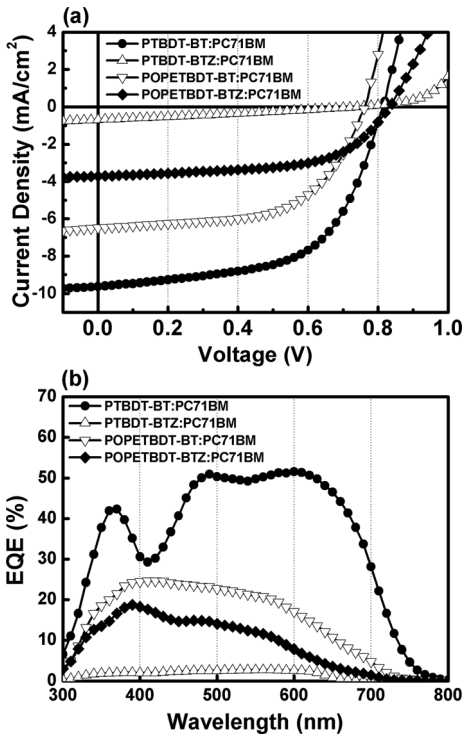

Fig. 4 (a) *J*–*V* characteristics of the polymer:$PC_{71}BM$ solar cells (AM 1.5G, 100 mW cm^{-2}) and (b) EQE curves of the corresponding polymer solar cells.

Photovoltaic properties

The photovoltaic characteristics of the synthesized polymers were investigated by fabricating devices with the structure of ITO/MoO_3/polymer:$PC_{71}BM$/LiF/Al. Fig. 4 shows the *J*–*V* characteristics of devices under AM 1.5 conditions with an intensity of 100 mW cm^{-2}. The best electrical properties achieved under various conditions are summarized in Table 2. The **PTBDT-BT**:$PC_{71}BM$ 1 : 1 (w/w) blend device with a thickness of 120 nm showed the best performance, with a V_{oc} of 0.81 V, a J_{sc} of 8.86 mA cm^{-2}, a FF of 47.9%, and a PCE of 3.44%. The **PTBDT-BTZ**:$PC_{71}BM$, **POPEBDT-BT**:$PC_{71}BM$, and **POPEBDT-BTZ**:$PC_{71}BM$ devices showed the best performances at 1 : 4 (w/w) blend ratios, thicknesses of 75–85 nm, and without any post-treatments.

As shown in Fig. 4, all devices comprising the polymers exhibited high V_{oc} values of 0.73–0.92 V. Although the origin of the V_{oc} remains the subject of debate, it is widely accepted that the energy difference between the HOMO of the donor and the LUMO of the acceptor determines the built-in potential of a device and, consequently, the values of V_{oc}.[34] As shown in Fig. 3, the synthesized polymers possessed deep HOMO energy levels relative to P3HT (−5.0 eV). Moreover, the highest values of V_{oc} achieved in the devices displayed a similar trend as a function of the HOMO levels of the donor polymers. The values of V_{oc} achieved in this study were attributed to the deep HOMO energy levels of the polymers, possibly due to the extended delocalization of BDT units upon the introduction of conjugated substituents. The slight differences between the properties of **PTBDT-BT** and **POPEBDT-BT** could be explained in terms of the different optimal compositions of the photoactive layers, 1 : 1 for **PTBDT-BT** and 1 : 4 for **POPEBDT-BT**.[35]

The generation of photocurrent from organic photovoltaic (OPV) cells using the synthesized polymers was investigated by comparing the external quantum efficiencies (EQE) of the devices. The measured EQE values agreed well with the measured J_{sc} values from the *J*–*V* curves, as shown in Fig. 4(b). The calculated J_{sc} values from the EQE obtained under AM 1.5 solar illumination differed only slightly (<5%) from the measured values. In principle, photocurrent generation depends directly on the product of light absorption, exciton separation, and charge collection. Because all synthesized polymers showed similar LUMO energy levels (Fig. 3), the exciton dissociation at the polymer–$PC_{71}BM$ interface should have minor effects on the generation of charge carriers.[36] In this regard, variations in

Table 2 Photovoltaic properties of polymer solar cells incorporating polymer:$PC_{71}BM$ blends

Polymer	Interfacial layer	Polymer : $PC_{71}BM$ (weight ratio)	V_{OC} (V)	J_{SC} (mA cm^{-2})	FF (%)	PCE (%)
PTBDT-BT[a]	LiF	1 : 1	0.81	8.86	47.9	3.44
	ZnO-PEG	1 : 1	0.81	9.62	59.2	4.61
PTBDT-BTZ	LiF	1 : 4	0.92	0.04	35.5	0.013
	ZnO-PEG	1 : 4	0.74	0.68	27.9	0.14
POPEBDT-BT	LiF	1 : 4	0.73	4.16	51.3	1.56
	ZnO-PEG	1 : 4	0.74	6.49	54.9	2.91
POPEBDT-BTZ	LiF	1 : 4	0.83	2.39	57.1	1.14
	ZnO-PEG	1 : 4	0.83	3.71	58.2	1.82

[a] With 3 vol% DIO.

the photovoltaic performance resulted from differences in the optical absorption, phase separation, and charge transport properties of the polymers.

The charge transport properties of the synthesized polymers affected the solar cell efficiency. These effects were investigated by measuring the space charge limited current (SCLC) mobility for each polymer. As shown in Fig. S6,† the measured hole mobilities were 1.93×10^{-3} cm^2 V^{-1} s^{-1} for **PTBDT-BT**, 4.34×10^{-5} cm^2 V^{-1} s^{-1} for **PTBDT-BTZ**, 4.82×10^{-4} cm^2 V^{-1} s^{-1} for **POPEBDT-BT** and 5.66×10^{-4} cm^2 V^{-1} s^{-1} for **POPEBDT-BTZ**. In general, an imbalance between electron and hole mobilities can promote the accumulation of space charge in BHJ structures, which results in the insufficient extraction of photo-generated charge.[37] The devices would then exhibit a low fill factor (FF) (<40%) with a higher series resistance and leakage current.[8,38–40] The devices prepared from each polymer except for **PTBDT-BTZ** showed relatively high FFs (>55%) under optimal conditions. These results indicated that within the range of the measured hole mobilities, the balance between each type of carrier transport did not play an important role in the photo-generation of current.

The effects of the optical absorption were investigated by measuring the absorption coefficients (α) of the synthesized polymers. **PTBDT-BT** displayed the highest maximum among the polymers, an α of 650 nm, which was one order of magnitude higher than the value for **PTBDT-BTZ** and twice the values of α for **POPEBDT-BT** and **POPEBDT-BTZ** (Fig. S7†). These results agreed well with the measured current densities of the devices, as shown in Table 2. Although **POPEBDT-BTZ** displayed a higher maximum α than **POPEBDT-BT**, the current density was higher for **POPEBDT-BT**. This discrepancy could be explained in terms of the development of phase separation and morphological variations within the photoactive layers. As shown in Table 1, the difference of the surface energies of the polymers to the $PC_{71}BM$ (34.2 mJ m^{-2}) is higher in the case of **POPEBDT-BT**. Since the polymers exhibited no particular crystallinity (Fig. S4†), the weak interactions between the polymer chains may have provided a well-mixed D–A phase in the blend films without the need for post-treatments. The differences between the surface energies of the donor and acceptor phases could have provided a strong driving force for spontaneous phase separation during the film-forming process, possibly by providing well-developed bicontinuous carrier transport pathways other than well-mixed blend structures.[8,41,42]

The photovoltaic performance of the **PTBDT-BT**:$PC_{71}BM$ blend could be optimized by adding 1,8-diiodooctane (DIO), a solvent additive with selective solubility for $PC_{71}BM$, to the blend solution prior to film deposition. **PTBDT-BT** has a surface energy (33.69 mJ m^{-2}) similar to that of $PC_{71}BM$; therefore, the materials initially formed a well-mixed blend structure. By contrast, the presence of the additive induced the chains of the donor polymer to self-aggregate, resulting in the spontaneous separation of donor and acceptor phases.[42–44] The photovoltaic performance of the **PTBDT-BT**:$PC_{71}BM$ blend in the presence of DIO exhibited a 20% increase in the photocurrent with a slight decrease (0.04 V) in V_{oc}; however, because the other polymers also displayed low surface energies, the presence of DIO in the blend solutions produced dramatic phase separation in the blend films, especially in **PTBDT-BTZ** and **POPEBDT-BT**. Aside from the obvious increase in the surface roughness (Fig. 5), micron-scale aggregation and dewetting behavior prevailed upon DIO addition (Fig. 6). As a result, photovoltaic properties were not observed.

Finally, the effects of interfacial layers on device performance were investigated. A solution of PEGylated ZnO nanoparticle

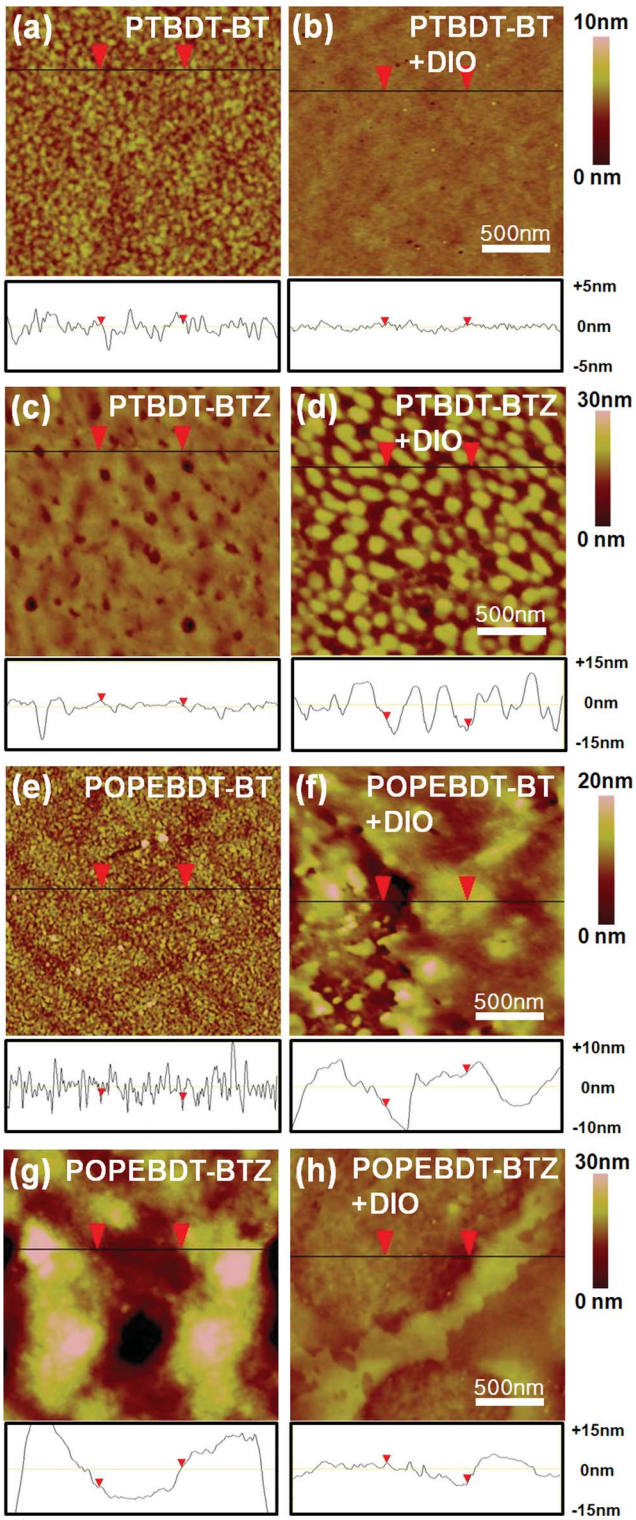

Fig. 5 AFM topography images of polymer:$PC_{71}BM$ blend films.

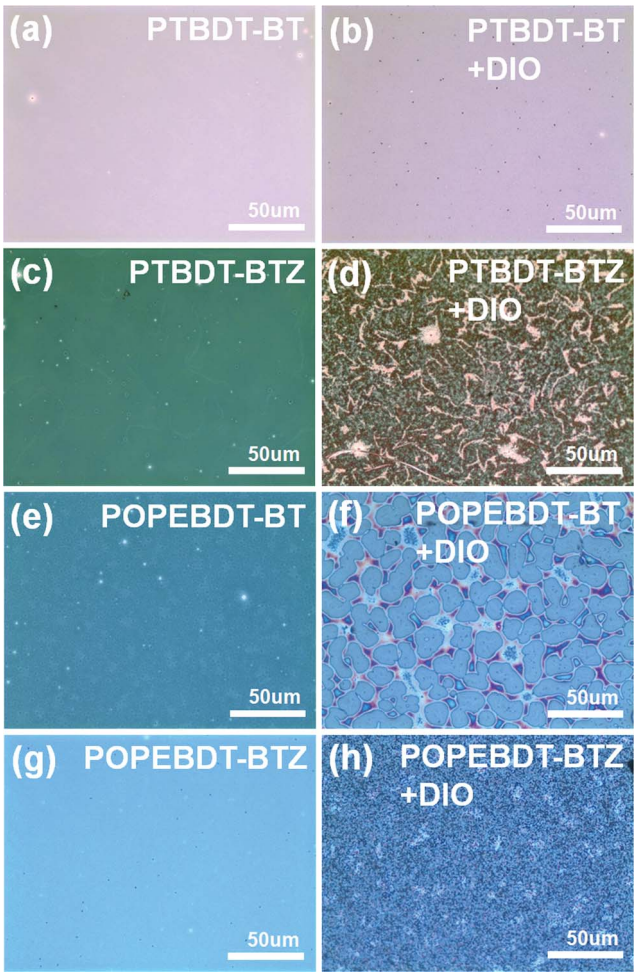

Fig. 6 Optical microscopy images of polymer:$PC_{71}BM$ blend films.

(10 nm) in 1-butanol was deposited onto the active layer to a thickness of 45 nm.[33] The resultant **PTBDT-BT** device showed an enhanced performance, with a V_{oc} of 0.81 V, a J_{sc} of 9.62 mA cm^{-2}, a FF of 59.2%, and a PCE of 4.61%. The deep HOMO energy level of ZnO and the high electron mobility resulted in higher FFs and shunt resistances.[45] The redistribution of the optical electric field could be estimated using optical simulation methods (Fig. S1†).[33,36,45,46] The optical electric field intensities inside the active layers formed from each synthesized polymer were observed to increase. Devices that used MoO_3 as a hole transport layer (HTL) benefitted from the internal field and FF relative to devices that used PEDOT:PSS as the HTL. This observation was attributed to the enhanced energy level alignment at the interface in this particular system comprising donor polymers with deep HOMO energy levels.[47] Further studies of these phenomena will be conducted in the future.

4. Summary and conclusions

Four new BDT derivative-based D–A alternating copolymers, **PTBDT-BT**, **PTBDT-BTZ**, **POPEBDT-BT**, **POPEBDT-BTZ**, were designed and synthesized by Stille coupling reaction. Polymers with small band gaps and deep HOMO energy levels (−5.42 eV for **PTBDT-BT**, −5.91 eV for **PTBDT-BTZ**, −5.58 eV for **POPEBDT-BT**, and −5.64 eV for **POPEBDT-BTZ**) were achieved by introducing TIPS and 4-octylphenylethynyl substituents onto the BDT unit. The photovoltaic performances of the synthesized polymers were investigated using the device configuration ITO/MoO_3/polymer:$PC_{71}BM$/ZnO/Al. **PTBDT-BT** exhibited the best photovoltaic performance in the series, with a J_{sc} of 9.62 mA cm^{-2}, a V_{oc} of 0.81 V, a FF of 59.2%, and a PCE of 4.61% due to the highest hole mobility (1.93×10^{-3} cm^2 V^{-1} s^{-1}), the high absorption coefficients, and an excellent BHJ morphology.

Acknowledgements

This work was supported by a grant (code no. 2011-0031628) from the Center for Advanced Soft Electronics under the Global frontier Research Program of the Ministry of Education, Science and Technology, Korea.

References

1 S. Günes, H. Neugebauer and N. S. Sariciftci, *Chem. Rev.*, 2007, **107**, 1324.
2 C. J. Brabec, N. S. Sariciftci and J. C. Hummelen, *Adv. Funct. Mater.*, 2001, **11**, 15.
3 B. C. Thompson and J. M. J. Fréchet, *Angew. Chem., Int. Ed.*, 2008, **47**, 58.
4 G. Yu, J. Gao, J. C. Hummelen, F. Wudl and A. J. Heeger, *Science*, 1995, **270**, 1789.
5 J. S. Kim, J. H. Lee, J. H. Park, C. Shim, M. Sim and K. Cho, *Adv. Funct. Mater.*, 2011, **21**, 480.
6 H.-C. Liao, C.-S. Tsao, T.-H. Lin, C.-M. Chuang, C.-Y. Chen, U.-S. Jeng, C.-H. Su, Y.-F. Chen and W.-F. Su, *J. Am. Chem. Soc.*, 2011, **133**, 13064.
7 J.-H. Kim, J. H. Park, J. H. Lee, J. S. Kim, M. Sim, C. Shim and K. Cho, *J. Mater. Chem.*, 2010, **20**, 7398.
8 J. S. Kim, Y. Lee, J. H. Lee, J. H. Park, J. K. Kim and K. Cho, *Adv. Mater.*, 2010, **22**, 1355.
9 B. Lim, J. Jo, S.-I. Na, J. Kim, S.-S. Kim and D.-Y. Kim, *J. Mater. Chem.*, 2010, **20**, 10919.
10 (*a*) H. J. Son, F. He, B. Carsten and L. Yu, *J. Mater. Chem.*, 2011, **21**, 18934; (*b*) H. Zhou, L. Yang and W. You, *Macromolecules*, 2012, **45**, 607.
11 Z.-G. Zhang and J. Wang, *J. Mater. Chem.*, 2012, **22**, 4178.
12 N. Blouin, A. Michaud and M. Leclerc, *Adv. Mater.*, 2007, **19**, 2295.
13 R. C. Coffin, J. Peet, J. Rogers and G. C. Bazan, *Nat. Chem.*, 2009, **1**, 657.
14 J. Hou, M.-H. Park, S. Zhang, Y. Yao, L.-M. Chen, J.-H. Li and Y. Yang, *Macromolecules*, 2008, **41**, 6012.
15 Y. Liang, D. Feng, Y. Wu, S.-T. Tsai, G. Li, C. Ray and L. Yu, *J. Am. Chem. Soc.*, 2009, **131**, 7792.
16 M. Yang, B. Peng, B. Liu, Y. Zou, K. Zhou, Y. He, C. Pan and Y. Li, *J. Phys. Chem. C*, 2010, **114**, 17989.
17 Y. Zhang, S. K. Hau, H.-L. Yip, Y. Sun, O. Acton and A. K.-Y. Jen, *Chem. Mater.*, 2010, **22**, 2696.
18 Y. Zou, A. Najari, P. Berrouard, S. Beaupré, B. R. Aïch, Y. Tao and M. Leclerc, *J. Am. Chem. Soc.*, 2010, **132**, 5330.
19 C. Piliego, T. W. Holcombe, J. D. Douglas, C. H. Woo, P. M. Beaujuge and J. M. J. Fréchet, *J. Am. Chem. Soc.*, 2010, **132**, 7595.
20 H.-Y. Chen, J. Hou, S. Zhang, Y. Liang, G. Yang, Y. Yang, L. Yu, Y. Wu and G. Li, *Nat. Photonics*, 2009, **3**, 649.
21 J. E. Anthony, D. L. Eaton and S. R. Parkin, *Org. Lett.*, 2002, **4**, 15.
22 Y. Li, Y. Wu, P. Liu, Z. Prostran, S. Gardner and B. S. Ong, *Chem. Mater.*, 2007, **19**, 418.
23 Y. Wang, S. R. Parkin and M. D. Watson, *Org. Lett.*, 2008, **10**, 4421.
24 P. Sista, H. Nguyen, J. W. Murphy, J. Hao, D. K. Dei, K. Palaniappan, J. Servello, R. S. Kularatne, B. E. Gnade, B. Xue, P. C. Dastoor, M. C. Biewer and M. C. Stefan, *Macromolecules*, 2010, **43**, 8063.

25 L. Huo, J. Hou, S. Zhang, H.-Y. Chen and Y. Yang, *Angew. Chem., Int. Ed.*, 2010, **49**, 1500.
26 L. Huo, S. Zhang, X. Guo, F. Xu, Y. Li and J. Hou, *Angew. Chem., Int. Ed.*, 2011, **50**, 9697.
27 Q. Shi, H. Fan, Y. Liu, W. Hu, Y. Li and X. Zhan, *Macromolecules*, 2011, **44**, 9173.
28 L. Biniek, S. Fall, C. L. Chochos, D. V. Anokhin, D. A. Ivanov, N. Leclerc, P. Lévêque and T. Heiser, *Macromolecules*, 2010, **43**, 9779.
29 W.-Y. Wong, X.-Z. Wang, Z. He, K.-K. Chan, A. B. Djurišić, K.-Y. Cheung, C.-T. Yip, A. M.-C. Ng, Y. Y. Xi, C. S. K. Mak and W.-K. Chan, *J. Am. Chem. Soc.*, 2007, **129**, 14372.
30 M. Thelakkat and H.-W. Schmidt, *Adv. Mater.*, 1998, **10**, 219.
31 R. S. Ashraf, M. Shahid, E. Klemm, M. Al-Ibrahim and S. Sensfuss, *Macromol. Rapid Commun.*, 2006, **27**, 1454.
32 W. J. E. Beek, L. H. Slooff, M. M. Wienk, J. M. Kroon and R. A. J. Janssen, *Adv. Funct. Mater.*, 2005, **15**, 1703.
33 S. B. Jo, J. H. Lee, M. Sim, M. Kim, J. H. Park, Y. S. Choi, Y. Kim, S.-G. Ihn and K. Cho, *Adv. Energy Mater.*, 2011, **1**, 690.
34 C. J. Brabec, A. Cravino, D. Meissner, N. S. Sariciftci, T. Fromherz, M. T. Rispens, L. Sanchez and J. C. Hummelen, *Adv. Funct. Mater.*, 2001, **11**, 374.
35 J. Liu, Y. Shi and Y. Yang, *Adv. Funct. Mater.*, 2001, **11**, 420.
36 P. Peumans, A. Yakimov and S. R. Forrest, *J. Appl. Phys.*, 2003, **93**, 3693.
37 P. W. M. Blom, V. D. Mihailetchi, L. J. A. Koster and D. E. Markov, *Adv. Mater.*, 2007, **19**, 1551.
38 C. Melzer, E. J. Koop, V. D. Mihailetchi and P. W. M. Blom, *Adv. Funct. Mater.*, 2004, **14**, 865.
39 M. A. Lampert and P. Mark, *Current Injection in Solids*, Academic Press, New York, 1970.
40 V. D. Mihailetchi, J. Wildeman and P. W. M. Blom, *Phys. Rev. Lett.*, 2005, **94**, 126602.
41 M. Campoy-Quiles, T. Ferenczi, T. Agostinelli, P. G. Etchegoin, Y. Kim, T. D. Anthopoulos, P. N. Stavrinou, D. D. C. Bradley and J. Nelson, *Nat. Mater.*, 2008, **7**, 158.
42 J. Peet, J. Y. Kim, N. E. Coates, W. L. Ma, D. Moses, A. J. Heeger and G. C. Bazan, *Nat. Mater.*, 2007, **6**, 497.
43 A. J. Moulé and K. Meerholz, *Adv. Funct. Mater.*, 2009, **19**, 3028.
44 S. B. Jo, W. H. Lee, L. Qiu and K. Cho, *J. Mater. Chem.*, 2012, **22**, 4244.
45 A. Moliton and J.-M. Nunzi, *Polym. Int.*, 2006, **55**, 583.
46 J. Gilot, I. Barbu, M. M. Wienk and R. A. J. Janssen, *Appl. Phys. Lett.*, 2007, **91**, 113520.
47 F. Zhang, M. Ceder and O. Inganäs, *Adv. Mater.*, 2007, **19**, 1835.